Trends in Applied Sciences Research

ISSN 1819-3579

Academic
Journals Inc.

www.academicjournals.com

Trends in Applied Sciences Research 6 (10): 1230-1237, 2011
ISSN 1819-3579 / DOI: 10.3923/tasr.2011.1230.1237

Extracting X-ray Reflectivity Profile of ZnO Thin Film using Atomic Force Microscopy Data

[1]Gh. Solookinejad and [2]M. Jabbari
[1]Department of Physics, Marvdasht Branch, Islamic Azad University, Marvdasht, Iran
[2]Department of Eletronic, Marvdasht Branch, Islamic Azad University, Marvadsht, Iran

Corresponding Author: Gh. Solookinejad, Department of Physics, Marvdasht Branch, Islamic Azad University, Marvdasht, Iran

ABSTRACT

Zinc Oxide (ZnO) thin film is a very important material for many different applications in both microelectronic and optoelectronic devices. In this study, surface structure of ZnO thin film, prepared by sol-gel spin coating method, was investigated. After thin film preparation, sample was taken out for *ex situ* AFM measurements to study the surface structure. Simulated X-Ray Reflectivity (XRR) of sample was extracted from Atomic Force Microscopy (AFM) data. Surface parameters such as Root Mean Squre (RMS) roughness, roughness exponent and correlation length, extracted from AFM, showed acceptable agreement with the parameters extracted from the simulated X-ray reflectivity method.

Key words: Roughness, surface parameters, atomic force microscopy, correlation length

INTRODUCTION

Over the last few years there has been a renewed interest in ZnO based electronic and optoelectronic devices and the significance of ZnO in the development of blue and ultraviolet optical devices was revealed (Marotti *et al*., 2008). ZnO thin films preparation has been an active field of study due to applications in transducers and catalysts since 1960s (Wang, 2004). Moreover, quasi two dimensional ZnO films have been produced for possible applications in surface and bulk acoustic wave devices for filtering (Hickernell, 2009) and sensing (Rozati and Akesteh, 2007), with the aim of use in accelerometers, force sensors and microphones (Itoh and Suga, 1993). ZnO thin films exhibit different transparency, conductivity and surface morphology, depending on the deposition technique. By employing different deposition techniques, piezoelectric properties of ZnO thin films have been investigated (Muthukumar *et al*., 2001). ZnO has been considered as an alternative to Indium Tin Oxide (ITO) for applications in display industry due to its acceptable transparency in visible light and its appropriate conduction properties (Avendano *et al*., 2006). Also optoelectronic applications of ZnO systems such as Light-Emitting Diodes (LEDs), photo detectors, electroluminescence devices, solar cells and ultraviolet lasers have recently attracted significant attention (Fu *et al*., 2009; Plank *et al*., 2009).

The influence of substituting low concentration Al at Zn site in ZnO thin films were investigated by Abdullah *et al*. (2009a). Also they simulated single layer Anti-reflective coating on silicon solar cell used on the refractive index limit of Zinc Oxide (Abdullah *et al*., 2009b). The structural and morphological properties of Sn doped ZnO thin films, deposited by spray pyrolysis and chemical bath deposition techniques, were investigated by Baneto *et al*. (2010). Percentage of color removal using coagulation as pretreatment, followed by the effect of ZnO, pH, stirring time

and solar photocatalytic as a final treatment has been examined by Makhtar *et al.* (2010). The microstructure, electrical properties and density of ZnO based varistor ceramics with different CuO content were investigated by Mansour *et al.* (2011).

For the reason of several new applications of ZnO, there has been a great deal interest in epitaxial ZnO thin films (Jin *et al.*, 2005). Production of ZnO thin films can be obtained using different techniques, e.g., PVD (physical vapor deposition) (Zhou *et al.*, 2004), CVD (chemical vapor deposition) (Purica *et al.*, 2002), metal organic chemical vapor deposition (Ye *et al.*, 2005), spray pyrolysis (Rozati and Akesteh, 2007), sputtering (Hsu *et al.*, 2008) and sol-gel processing (Shao *et al.*, 2006). Because of low cost and appropriate features, sol-gel technique competes with other techniques.

Atomic Force Microscopy (AFM) scans a sample under a tip with a radius of between 10 and 40 nm at the end of a soft cantilever. In contact mode AFM the tip senses the surface topography monitored by the detection of a laser beam from the back of the cantilever onto a photo detector that is sensitive to position. A feedback loop is employed to manage the vertical position of the sample mounted on a piezoelectric tube, maintaining the constant force between the tip and sample surface and thus measuring the surface topography. The vertical space traveled by the scanner at each x and y data point is stored by the computer to form the topographic image of the sample surface (Magonov and Reneker, 1997). Because of high lateral resolution of this procedure and its potential of gaining quantitative three-dimensional information concerning surface topography, roughness, height and the tilt angle of topographic structures, this procedure is appropriate for the investigation of thin film surfaces. This technique provides helpful numerical data of surface height at digitized locations on the film. A number of analyses have been developed to utilize the data such as, Power Spectrum Density (PSD) (Suresh *et al.*, 2004) and fractal analysis (Park *et al.*, 2009). This study reports the results of computation of x-ray reflectivity on the basis of AFM measured surface profiles for ZnO thin film. These calculations allowed us to estimate the effective correlation length of roughness, roughness exponents and rms roughness which determine scattering of x-ray radiation by surface.

MATERIALS AND METHODS

Thin film preparation: ZnO thin film was prepared by sol-gel spin coating method onto glass substrate with 3000 rpm for 45 sec. After each coating, the film was preheated at 275°C for 10 min and post heated at 450°C for 80 min. The deposition was repeated to obtain a film with proper thickness.

Atomic force microscopy: *Ex situ* measurements of surface morphology of the film was carried out following heating process. For obtaining surface morphology of thin films we used an Atomic Force Microscopy (AFM) instrument (TM Microscopes Veeco Metrology Group) on contact mode. A commercial standard pyramidal Si3N4 tip was used. AFM image was acquired in ambient air and digitized in to 256×256 pixels. AFM image of ZnO thin film is shown in Fig. 1.

As can be seen, a typical morphological feature is recognized readily by visual inspection of Fig. 1. This is that the granules of various scales exist in film and is distributed evenly in some range. In addition the granules represent different irregular shapes, sizes and separations. A number of algorithms have been employed in order to determine the value of fractal dimension D_f based upon AFM images such as box-counting and fractal analysis. In order to study the fractal properties of ZnO thin film, we computed the height-height correlation functions of sample from AFM data. Statistical analysis can quantitatively check the characteristics of the surface morphology and study kinetic growth procedure. From height-height correlation function of the

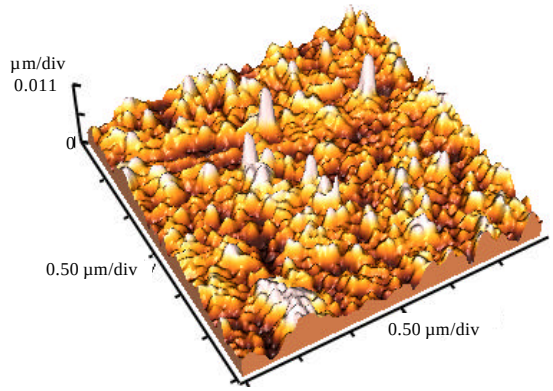

Fig. 1: AFM images of ZnO thin films prepared by spin coating method

surface we can conclude the rms of surface roughness, roughness exponent and the lateral correlation length. This result will be compared with the result of x-ray reflectivity simulation.

RESULTS AND DISCUSSION

At first, using AFM images of sample surfaces, the correlation length and fractal dimensionality of roughness were estimated for each substrate. For this purpose, using the Fourier transformation, a spectral power density of surfaces (PSD) was calculated:

$$PSD(k_x,k_y)=\frac{1}{S}\left|F[Z(x,y)]\right|^2 \quad (1)$$

Then two dimensional height-height correlation function C (X, Y) was computed via reverse Fourier transformation:

$$C_{AFM}(X,Y)=F^{-1}[PSD(k_x,k_y)] \quad (2)$$

The lateral correlation length of roughness ρ_{AFM} was determined as a distance; where the correlation function is reduce e times. For estimating the fractal dimensionality of surfaces we used the variation method, wherein the superior performance of this method compared to over common D_F-evaluating algorithms. According to the variation method, for a sequence of dilative square regions which had a 2n×2n size and were centered at point (i, j), averaged-over-M^2-points variation of the highest and lowest values of height was determined:

$$V_n=\frac{1}{M^2}\sum_{i,j}[Z^{max}_{i,j}-Z_{i,j}^{min}] \quad (3)$$

where, M = N-2n. In order to calculate the fractal dimensionality, we plotted dependence of $In[(N/n)^3V_n]$ on In(N/n) for n = 1,2,... n_{max}. The slope of this graph in the linear region gives the value of fractal dimensionality. If one knows the fractal dimension of a surface, one can derive the Herst parameter by the formula:

$$D = 3-h \quad (4)$$

Secondly, by using the profiles of surface derived by AFM for sample we calculated angular dependencies of specularly reflected intensity. The Distorted-wave Born approximation was used. Following Sinha *et al.* (1988), a differential cross section for the diffuse component of reflected radiation is written:

$$\left(\frac{d\sigma}{d\Omega}\right)_{diff} = \left\langle \frac{\left|k_0{}^2(1-n^2)\right|}{16\pi^2} \left|T(k_1)\right|^2 \left|T(k_2)^2\right| \left|F(q_t)\right|^2 \right\rangle \tag{5}$$

$$F(q_t) = \frac{i}{q_z{}^t} \iint_s dxdy(\exp(-iq_z{}^t Z(x,y)) - 1)\exp(i(q_x x + q_y y))$$

where, T (k) is the Fresnel transmittance, $k_{1,2}$ the wave vectors of incident and scattered waves, $k_0 = 2\pi/\Omega$, q_t is the difference of the wave vectors transfer in medium and n the refractive index of medium. The intensity of radiation scattered into the detector which is observed at a solid angle $\Delta\Omega$ from the point of radiation incidence on the sample, is given by the expression:

$$I_{diff} = I_0 \frac{\Delta\Omega}{A}\left(\frac{d\sigma}{d\Omega}\right) \tag{6}$$

where, I_0 is the intensity of incident beam and A is the area of the beam. If we substitute the AFM profile of surface Z = Z (x,y) in the Eq. 5 we can calculate the angular dependence of the reflected intensity. Figure 2 shows X-ray reflectivity derived numerically for sample. Due to the interference of reflected waves which are reflected from different interfaces within a thin film, intensity oscillations in the reflecticity can be observed. The periodicity in reflectivity profile can be related to the thickness of the film. Roughness of the surface can be taken into account in the same fashion in the Fresnel coefficients, provided that the roughness is small compared to thicknesses of the film. Both the position of the critical angle and the period of the interference have been indicated in the

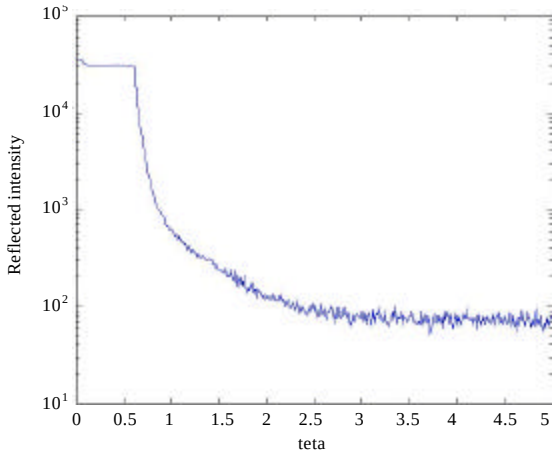

Fig. 2: X-ray reflectivity derived numerically for sample

simulated X-ray reflectivity. We can use this information for extracting structural parameters of the film.

Parameters σ, D_f and h were estimated by means of approximation of real surfaces by effective self-affine Gaussian surfaces. Equation 5 in this case can be written in the following form:

$$\left(\frac{d\sigma}{d\Omega}\right)_{diff} = \frac{\left|k^2{}_0(1-n^2)\right|^2}{16\pi^2}\left|T(k_1)\right|\left|T(k_2)\right|^2 S(q_t), \tag{7}$$

$$S(q_t) = \frac{\exp(-((q^t{}_z)^2 + (q^{t*}{}_z)^2\sigma^2/2)}{\left|q^t{}_z\right|^2}\iint_{S_0} dXdY(\exp(\left|q^t{}_z\right|^2 C(X,Y)) - 1)\exp(i(q_x X + q_y Y))$$

Here the height-height correlation function of roughness C (X,Y) was determined in the following way:

$$C(X,Y) = \sigma^2 e^{-\left(\frac{\sqrt{X^2+Y^2}}{\rho}\right)^{2h}} \tag{8}$$

Parameters of surface roughness are listed in Table 1.

Where, h is the roughness exponent which describes how locally "wiggly" the sample surface is, σ is the rms of surface roughness and ρ is the lateral correlation length which is defined as the largest distance in which the height is still correlated. The relationship between roughness exponent h and fractal dimension D_f is $D_f = E+1-h$ with $0<h<1$, where E+1 is the dimension of the embedded space. Fractal dimension $D_f$describes the total profile complexity and takes into account the changes of the normalized profile length as a function of the observation scale. The value of D_f can theoretically change from 2 for a flat profile to 3 for profiles which fill whole area defined by the square constructed by height roughness. If the $D_f$value is between 2 and 3, then the analyzed profiles have some fractal properties. If the fractal dimension is higher, it suggests that the profile complexity is more pronounced. Also larger value of h corresponds to a locally flat surface structure while a smaller one corresponds to more locally rough morphology. Surface structural parameters σ, h and ρ are independent from each other and they vary according to the process by which the surface morphology is formed. These parameters completely characterize a self-affine surface. As can be seen from Table 1, for this sample the parameters of roughness, estimated from AFM and simulated XRR, are quite comparable. For essentially non-Gaussian surfaces, the mean-square roughness estimated from the AFM data exceed the XRR estimation. In the angular range of interest x-ray radiation is sensitive to relatively low spatial frequencies. But in fact, there are intensive high frequency components in the spatial spectrum of surface. Existence of high frequency components which are absent in the model surface, is the reason why the distance, where the points of surface correlate with each other, is shorter in comparison with the correlation length estimated from the XRR experiment.

Table 1: Parameters of surface roughness found from and AFM data and simulated XRR

[1]σ_{AFM} (nm)	σ_{XRR} (nm)	[2]h_{AFM}	h_{XRR}	[3]ρ_{AFM}	ρ_{XRR}
2.3±0.2	2.6±0.1	0.89±0.1	0.93±0.1	56.2±1	62.1±1

[1]σ is the rms of surface roughness, [2]h is the roughness exponent, [3]ρ is the lateral correlation length

On the other hand, using the same procedure as in XRR experiments, parameters of surface roughness were estimated from the rocking curve calculated on the basis of AFM data. These effective parameters, as can be seen from Table 1, are in good agreement with XRR estimations for sample.

The Phase-Sensitive Acoustic Microscopy (PSAM) and Atomic Force Microscopy (AFM) techniques for characterizing polymer thin films has been applied by Ngwa *et al.* (2005). Their evaluation was based on results from three-dimensional vector contrast imaging for PSAM and multimodal imaging for AFM. AFM imaging has been applied to study the structural properties of polycrystalline $CuInSe_2$ films by Alberts (2000) which are usually used as absorber materials in thin film solar cell mechanisms. The outcomes were applied to evaluate the particular thin film growth schemes in terms of producing device quality material for solar cell applications. Coupeau and Grilhe (2001) carried out *in situ* atomic force microscopy observations of deformed (under stress) materials on both single crystals and thin films on substrates. Tsay *et al.* (2010) investigated the effect of the heating rate of the preheating process on the surface morphology and optical properties of sol-gel derived ZnO thin films. Their experimental results show that the heating rate of the preheating process robustly affected the surface morphology and transparency of ZnO thin film.

CONCLUSION

In present study, a procedure which permits calculation of the angular dependencies of reflectivity radiation scattered by a surface, was carried out. Effective parameters of roughness can be obtained using this procedure. Comparative AFM and simulated XRR examination of roughness was carried out for an ensemble of glass substrates. It is demonstrated that the effective parameters estimated by the proposed method are in good agreement with the parameters obtained from AFM data.

ACKNOWLEDGMENTS

The authors would like to thank the Office of Graduate Studies of the University of Isfahan for their support. Gh. Solookinejad would like to thank the Iranian Nanotechnology Initiative Council for their support.

REFERENCES

Abdullah, H., A. Lennie and I. Ahmad, 2009a. Modelling and simulation single layer anti-reflective coating of ZnO and ZnS for silicon solar cells using silvaco software. J. Applied Sci., 9: 1180-1184.

Abdullah, H., R. Silvia and J. Syarif, 2009b. Study of structure, surface morphology and optical property on ZnO: Al thin films as anti-reflecting coating. Asian J. Applied Sci., 2: 191-196.

Alberts, H., 2000. Atomic force microscopy imaging of polycrystalline CuInSe2 thin films. J. Microsci., 197: 206-215.

Avendano, E., L. Berggren, G.A. Niklasson, C.G. Granqvist and A. Azens, 2006. Electrochromic materials and devices: Brief survey and new data on optical absorption in tungsten oxide and nickel oxide films. Thin Solid Films, 496: 30-36.

Baneto, M., Y. Lare, L. Cattin, M. Addou and K. Jondo *et al.*, 2010. Comparison of the structural and morphological properties of Sn doped ZnO films deposited by spray pyrolysis and chemical bath deposition. Asian J. Mater. Sci., 2: 196-203.

Coupeau, C. and J. Grilhe, 2001. Atomic force microscopy observations of *in situ* deformed materials: Application to single crystals and thin films on substrates. J. Microsc., 203: 99-107.

Fu, Q., L. Hu, D. Yu, J. Sun, H. Zhang, B. Huo and Z. Zhao, 2009. ZnO thin films deposited by a CVT technique in closed ampoules. Mat. Lett., 63: 316-318.

Hickernell, F.S., 2009. DC triode sputtered zinc oxide surface elastic wave transducers. J. Appl. Phys., 44: 1061-1071.

Hsu, Y.H., J. Lin and W.C. Tang, 2008. RF sputtered piezoelectric zinc oxide thin film for transducer applications. J. Mater. Sci.: Mater. Electr., 19: 653-661.

Itoh, T. and T. Suga, 1993. Development of a force sensor for atomic force microscopy using piezoelectric thin films. Nanotechnol., 4: 218-218.

Jin, C., R. Narayan, A. Tiwari, H. Zhou, A. Kvit and J. Narayan, 2005. Epitaxial growth of zinc oxide thin films on silicon. Mat. Sci. Engin. B, 117: 348-354.

Magonov, S.N. and D.H. Reneker, 1997. Characterization of polymer surfaces with atomic force microscopy. Annu. Rev. Mater. Sci., 27: 175-222.

Makhtar, S.M.Z., N. Ibrahim and M.T. Selimin, 2010. Removal of colour from landfill by solar photocatalytic. J. Applied Sci., 10: 2721-2724.

Mansour, S.E., O.A. Desouky, S.M. Negim and W.A. Kamil, 2011. Microstructure and current-voltage characteristics of (ZnO-CuO) varistor system in the presence of additive oxides, Cr_2O_3, Bi_2O_3 and NiO. Curr. Res. Chem., 3: 29-48.

Marotti, R.E., C.D. Bojorge, E. Broitman, H.R. Canepa, J.A. Badan *et al.*, 2008. Characterization of Zno and Zno: Al thin films deposited by the sol-gel dip-coating technique. Thin Solid Films, 517: 1077-1080.

Muthukumar, S., N.W. Emanetoglu, G. Patounakis, C.R. Gorla, S. Liang and Y. Lu, 2001. Two-step metalorganic chemical vapor deposition growth of piezoelectric ZnO thin film on SiO_2/Si substrate. J. Vac. Sci. Technol. B, 19: 1850-1853.

Ngwa, W., W. Luo, A. Kamanyi, K.W. Fomba and W. Grill, 2005. Characterization of polymer thin films by phase sensitive acoustic microscopy and atomic force microscopy: A comparative review. J. Microsc., 218: 208-218.

Park, Y.B., S.W. Rhee and J.H. Hong, 2009. Growth and fractal scaling nature of copper thin films on Tin surface by metal organic chemical vapor deposition from hexafluoroacethylacetonate Cu vinyltrimethylsilane. J. Vac. Sci. Technol., B, 15: 1995-2000.

Plank, N.O.V., I. Howard, A. Rao, M.W.B. Wilson and C. Ducati *et al.*, 2009. Efficient Zno nanowire solid-state dye-sensitized solar cells using organic dyes and core-shell nanostructures. J. Phys. Chem. C, 113: 18515-18522.

Purica, M., E. Budianu, E. Rusu, M. Danila and R. Gavrila, 2002. Optical and structural investigation of Zno thin films prepared by chemical vapor deposition (CVD). Thin Solid Films, 403: 485-488.

Rozati, S.M. and S. Akesteh, 2007. Characterization of ZnO: Al thin films obtained by spray pyrolysis technique. Mat. Charact., 58: 319-322.

Shao, Z.B., C.Y. Wang, S.D. Geng, X.D. Sun and S.J. Geng, 2006. Fabrication of nanometer-sized zinc oxide at low decomposing temperature. J. Mater. Process. Technol., 178: 247-250.

Sinha, S.K., E.B. Sirota, S. Garoff and H.B. Stanley, 1988. X-ray and neutron scattering from rough surfaces. Phys. Rev. B Condens Matter, 38: 2297-2311.

Suresh, N., R. Thakur, D.M. Phase and S.M. Chaudhari, 2004. Interfacial electron density profile in Nb/Si bilayer films: An X-ray reflectivity study. Vacuum, 72: 419-426.

Tsay, C.Y., K.S. Fan, S.H. Chen and C.H. Tsai, 2010. Preparation and characterization of ZnO transparent semiconductor thin films by sol-gel method. J. Alloys Compounds, 495: 126-130.

Wang, Z.L., 2004. Zinc oxide nanostructures: Growth, properties and applications. J. Phys. Condensed Matter, 16: R829-R858.

Ye, J.D., S.L. Gu, F. Qin, S.M. Zhu and S.M. Liu *et al*., 2005. Correlation between green luminescence and morphology evolution of Zno films. Appl. Phys. A, 81: 759-762.

Zhou, Y., P.J. Kelly, A. Postill, O. Abu-Zeid and A.A. Alnajjar, 2004. The characteristics of aluminium-doped zinc oxide films prepared by pulsed magnetron sputtering from powder targets. Thin Solid Films, 447: 33-39.